American Journal of Pathology, Vol. 151, No. 1, July 1997

Reactive Oxygen Species Cause Direct Damage of Engelbreth-Holm-Swarm Matrix

Barbara Riedle and Dontscho Kerjaschki

From the Section of Ultrastructural Pathology, Institute of Clinical Pathology, University of Vienna, Vienna, Austria

Reactive oxygen species (ROS) are produced and released into the extracellular spaces in numerous diseases and contribute to development and progression, for example, of inflammatory diseases, proteinuria, and tumor invasion. However, little is known about ROS-induced chemical changes of interstitial matrix proteins and their consequences for the integrity of the matrix meshwork. As basement membranes and other matrices are highly cross-linked and complex, the relatively simple matrix produced by Engelbreth-Holm-Swarm (EHS) sarcoma, and proteins isolated therefrom, were incubated in vitro with defined concentrations of ROS that were generated by the Fenton or xanthine oxidase/xanthine reactions. This resulted in two countercurrent effects. Although up to ~15% of the EHS matrix proteins were released into the supernatant in a ROS dose-response relationship, the residual insoluble matrix was partially cross-linked by ROS. Matrix proteins released into the supernatants were examined by rotary shadowing, quantitative sodium dodecyl sulfate polyacrylamide gel electrophoresis, immunoblotting, and fluorospectrometry for loss of tryptophans and formation of bityrosine residues. At relatively low ROS concentrations, selective liberation of morphologically intact laminin/entactin was found that, however, failed to reassociate and showed oxidative damage of its tryptophan residues. At higher ROS concentrations, laminin and entactin were progressively disintegrated, partially fragmented, and eventually completely degraded. At this point oligomers of type IV collagen predominated in the supernatant, and proteoglycans were not encountered at any concentration of ROS. Similar gradual molecular changes were also obtained when fractions of isolated soluble EHS matrix proteins were incubated with graded concentrations of ROS. In these experiments, the formation of covalently linked oligomers and aggregates paralleled the ROS-dependent formation of cross-linking bityrosine groups. ROS scavengers pinpointed to the hydroxyl radical as the most damaging radical species. Protease inhibitor experiments suggested that degradation of matrix proteins was caused primarily by the direct action of ROS and not by proteolysis by potentially contaminating proteases. Collectively, these results provide evidence that EHS matrix proteins show differential sensitivity to ROS-induced damage in a reproducible, sequential pattern, in the order entactin > laminin > type IV collagen, and that ROS cause partial dissociation and cross-linking of the EHS matrix. (Am J Pathol 1997, 151:215–231)

Extracellular matrix and basement membranes are complex meshworks composed primarily of collagens, laminins, entactin, and proteoglycans. Despite this limited repertoire of molecular components, matrices come in large varieties and serve diverse functions, such as formation of barriers for migration of cells, reservoir of growth factors and cytokines, and many others.[1–3] A striking example of functional matrix specialization is the renal glomerular basement membrane (GBM) that constitutes the filtration barrier for plasma proteins.[4,5] In many glomerular diseases, loss of selective GBM permeability and consequent proteinuria are associated with structural damage of matrix proteins. Examples include genetic defects of type IV collagen in Alport syndrome,[6] damage inflicted by autoantibodies to type IV collagen in Goodpasture syndrome in humans,[7]

Supported by the SFB 05 (Microvascular Damage and Repair), Project 07, of the Austrian Research Fund (to D. Kerjaschki).

Accepted for publication April 3, 1997.

Address reprint requests to Dr. D. Kerjaschki, Department of Clinical Pathology, University of Vienna, AKH, Währinger Gürtel 18–20, A-1090 Vienna, Austria.

and genetic knock out of a single chain of s-laminin in mice.[8]

Physiological remodeling of extracellular matrix and basement membranes is regulated primarily by the balance of proteases and protease inhibitors and presumably also by locally produced reactive oxygen species (ROS) and their natural scavengers. We were interested in examining the effect of ROS on GBMs because previous work has established a causal relation with proteinuria in Heymann nephritis, a classical rat model disease for human membranous nephropathy.[9] Beyond this aspect, interactions of ROS with matrix proteins also occur and could be of relevance in several pathological conditions, such as acute and chronic inflammatory diseases and in liver[10] and myocardial damage.[11]

Little is known about direct ROS-induced molecular modifications of individual matrix proteins and their consequences for structure, properties, and functions of the matrix. This is due in part to technical limitations because of extensive cross-linking of matrix proteins, for example, by lysyl oxidase via collagens. Here we have examined *in vitro* effects of ROS on the matrix produced by Engelbreth-Holm-Swarm (EHS) sarcoma, an extensively studied and well characterized simple surrogate of basement membranes.[12] As the experimental accessibility of matrix proteins requires their solubility in sodium dodecyl sulfate (SDS), we have chosen to grow EHS tumors in lathyritic mice, in which cross-linking of collagen was suppressed by inhibition of the lysyl oxidase. This approach has revealed an unexpected differential sensitivity of matrix proteins to ROS.

Materials and Methods

Antibodies

Rat monoclonal IgG specific for laminin β1 and γ1 chains, EHS-entactin, and EHS-perlecan were obtained from Upstate Biotechnology (Lake Placid, NY). Affinity-purified rabbit anti-laminin-1 IgG was from Serotec (Stoughton, MA), and rabbit anti-EHS type IV collagen was from Chemicon (Temecula, CA).

Reagents

Ferrous chloride tetrahydrate, lyophilized xanthine oxidase, xanthine, choline chloride, mono- and dipotassium phosphate, 2,3-dihydroxybenzoate, allopurinol, EDTA-tetranatrium salt, deferoxamine mesylate, 1,1,3,3,-tetraethoxypropane, superoxide dismutase, catalase, L-methionine, 1,10-phenanthroline monohydrate, β-aminopropionitril, antipain hydrochloride, pepstatin A, leupeptin, Azocoll, and Sephadex G 100 were purchased from Sigma Chemical Co. (St. Louis, MO). H_2O_2 (30% Perhydrol), ammonium acetate, sodium benzoate, sodium salicylate, *o*-phosphoric acid, *N,N'*-dimethylthiourea (DMTU), and glycerol were obtained from Merck (Darmstadt, Germany). Bovine serum albumin was from Behring (Marburg, Germany). Triton X-100 (Surfact Amps, 10%), alkaline phosphatase substrates nitroblue tetrazolium chloride and 5-bromo-4-chloro-3-indolyl phosphate *p*-toluidine were from Pierce (Rockford, IL). Tris, SDS, dithiothreitol (DTT), ammonium persulfate, and Tween 20 were from BioRad (Richmond, CA). Alkaline-phosphatase-conjugated antibodies were from Promega (Madison, WI). Pefabloc was from Pentapharm AG (Basel, Switzerland). Quinine sulfate was from BDH (Poole, UK).

Generation and Calibration of ROS Produced by the Fenton and Xanthine Oxidase/Xanthine Reactions

Defined concentrations of ROS were produced *in vitro* by the Fenton reaction in TBS or PBS (pH 7.4) with protease inhibitors (0.5 mg/ml Pefablock and 2.5 μg/ml antipain, leupeptin, and pepstatin) at 4°C. The Fenton reaction was initiated and maintained by two strategies: 1) by addition of variable amounts of H_2O_2 (final concentrations of 0 to 1200 mmol/L) to fixed concentrations of Fe^{2+} (0.3 or 0.5 mmol/L) for constant incubation times (15 and 120 minutes) or 2) by addition of a constant amount of H_2O_2 (final concentrations of 50 mmol/L) to a set concentration of Fe^{2+} (0.3 mmol/L) and variable incubation intervals (0 to 120 minutes). ROS production was quantitated in pilot experiments in the absence of target proteins by detection of hydroxyl radicals by a fluorospectrometric benzoate method,[13] using quinine sulfate as standard (with 1 U equivalent to 0.01 μg of quinine sulfate),[14] or a spectrophotometric salicylate method with 2,3-dihydroxybenzoate (1 mmol/L to 1 μmol/L) as standard.[15] The complementary consumption of H_2O_2 was determined by iodometric titration using 4 mmol/L methionine as hydroxyl radical acceptor.

Xanthine oxidase purified from buttermilk was depleted of contaminating proteases by Sephadex G 100 size exclusion chromatography in choline buffer (125 mmol/L choline chloride, 25 mmol/L potassium phosphate), pH 7.4, containing 0.01 mmol/L EDTA.[16,17] Protease activity was determined by a photometric Azocoll method.[16] ROS were produced by incubation of 3 mU/ml xanthine oxidase with 1.2

mmol/L xanthine, 0.3 mmol/L Fe^{2+}, and 0.1 mmol/L EDTA to stabilize the enzyme and to enhance dismutation of the superoxide anion.[18] Superoxide anion was quantitated by a photometric time scan of the conversion of xanthine to urate at 295 nm in a Hitachi U 2000 spectrophotometer (Jasco, Tokyo, Japan).

Preparation of EHS Matrix

EHS sarcomas were induced in lathyritic C57/Bl mice by subcutaneous injection of tumor cells into the back thighs.[19] After 10 weeks, tumors with ~2 cm diameter were harvested. Aliquots were frozen and stored in liquid N_2. Tumors were pressed through a 315-mesh steel sieve, and fragments were collected by centrifugation, washed five times with 50 mmol/L Tris-buffered or phosphate-buffered saline (TBS or PBS), suspended by vortexing, and distributed into 100-μl aliquots containing 8 mg ± 5% protein. The use of mice in these experiments was permitted by the Animal Ethics Committee and the Austrian Ministry of Science.

Interaction of ROS with EHS Matrix

Aliquots of EHS matrix were suspended in TBS or PBS containing 0.3 mmol/L Fe^{2+}. The Fenton reaction was started by addition of H_2O_2 (final concentrations from 0 to 150 mmol/L; final volume, 1 ml). Incubation was carried out for 30 or 120 minutes at 4°C. The reaction was stopped by addition of DMTU (final concentration, 2.5 mmol/L). In control incubations, H_2O_2 was omitted. Solubilized proteins and undissociated matrix were separated by centrifugation for 5 minutes at ~12,000 × *g* in a microfuge (Hettich, Tuttlingen, Germany). A 750-μl volume of the supernatant was collected and recentrifuged. To avoid contamination by incompletely pelleted fragments of EHS matrix, aliquots of the supernatants were collected from the top of the tubes. They were used for determination of protein concentrations by the Coomassie Plus (Pierce) assay, for rotary shadowing, for trichloroacetic acid precipitation and SDS-polyacrylamide gel electrophoresis (SDS-PAGE), and for determination of oxidation of tryptophan residues.

Alternatively, aliquots of EHS matrix were suspended in PBS containing 0.3 mmol/L Fe^{2+} and 0.1 mmol/L EDTA and were incubated with xanthine oxidase (3 mU/ml) and xanthine (1.2 mmol/L) for 30 or 120 minutes at 4°C. The reaction was stopped by allopurinol (2 mmol/L). Supernatants were collected and processed as described above. In controls, aliquots of matrix were incubated without xanthine oxidase and xanthine or with xanthine oxidase without xanthine.

The pellets of EHS matrix remaining after 120 minutes of incubation with ROS (produced by the Fenton reaction, using 20 and 150 mmol/L H_2O_2 in TBS) or with TBS in controls were resuspended by vortexing and incubated in TBS containing 20 mmol/L EDTA for 1 hour at 20°C. After centrifugation for 5 minutes at ~12,000 × *g*, the concentration of proteins released into the supernatants by EDTA was determined by the Coomassie Plus assay.

Isolated Extracellular Matrix Proteins

Preparations of isolated EHS matrix proteins enriched for laminin were purchased from Biomedical Technologies. Composition and integrity of matrix proteins were monitored by rotary shadowing, SDS-PAGE, and immunoblotting. Batches were discarded when proteolytic degradation was observed after incubations for 2 hours at 4°C despite the presence of protease inhibitors.

Interaction of ROS with Isolated Matrix Proteins

Aliquots of soluble laminin-enriched matrix protein fractions (33 μg in 60 μl of TBS) were incubated in 0.5 mmol/L Fe^{2+} for 1 minute, followed by addition of increasing concentrations of H_2O_2 (0 to 1200 mmol/L final concentration). After 15 minutes at 4°C, the reaction was stopped by DMTU (final concentration, 35 mmol/L). Samples were processed for rotary shadowing, SDS-PAGE and laser densitometry, fluorospectrometry for tryptophan and tyrosine oxidation, and for determination of thiobarbituric-acid-reactive lipid peroxidation products.[20]

ROS-Induced Polymerization and Aggregate Formation of Matrix Proteins

Aliquots of soluble laminin-enriched matrix proteins fractions (120 μg in 85 μl of TBS) were incubated in 0.3 mmol/L Fe^{2+} for 1 minute, followed by addition of H_2O_2 (0.5 and 20 mmol/L) and incubation for 130 minutes at 37°C, to permit noncovalent polymerization[21] and/or covalent aggregate formation. In controls, H_2O_2 was omitted. The insoluble polymeric products were collected by centrifugation (6 minutes at ~12,000 × *g*), and the protein concentrations in the supernatants were determined by the Coomassie Plus assay. Proteins in the supernatant were also

examined by rotary shadowing and by fluorospectrometry for oxidation of tryptophan residues.

The pellets obtained in the control incubations and after treatment with 20 mmol/L H_2O_2 were incubated with 20 mmol/L EDTA for 1 hour at 20°C to dissociate noncovalent homotypic interactions of the laminin polymers. The concentration of EDTA-extracted proteins in the supernatants was determined by the Coomassie Plus assay. The EDTA-insoluble pellet obtained after incubation with 20 mmol/L H_2O_2 was further examined for its ability to dissolve in 5 mmol/L DTT and for the presence of malone dialdehyde by the thiobarbituric acid assay.[20]

ROS-Induced Derivatization of Tryptophan and Tyrosine Residues

Oxidative alterations of tryptophan and tyrosine residues were determined by fluorospectrometry in a Jasco spectrofluorometer 777 with 1 U equivalent to 0.01 μg of quinine sulfate.[14] Specific tryptophan fluorescence was detected at 280 nm excitation and 340 to 350 nm emission. Bityrosine formation was measured at 325 nm excitation and 415 nm emission.

Identification of Matrix-Damaging ROS by Use of Scavengers

Aliquots of soluble laminin-enriched matrix protein fractions (28 μg in 60 μl of 50 mmol/L TBS) were incubated in 1200 mmol/L H_2O_2 and 0.5 mmol/L Fe^{2+} for 15 minutes at 4°C, with one of the following scavengers: catalase (11,500 U/ml), superoxide dismutase (1600 U/ml), methionine (37 mmol/L), DMTU (168 mmol/L), or deferoxamine mesylate (75 μmol/L). The matrix proteins were analyzed by SDS-PAGE and rotary shadowing.

Inhibition of Endogenous Metalloproteases

To determine whether ROS-activated contaminating metalloproteases could play a role in matrix protein degradation, isolated matrix proteins (28 μg in 60 μl of TBS) were incubated in 1200 mmol/L H_2O_2 and 0.5 mmol/L Fe^{2+} for 15 minutes at 4°C, with the metal ion (Zn^{2+} and Ca^{2+}) chelator 1,10-phenanthroline (1 mmol/L).[22] The proteins were assayed by SDS-PAGE and rotary shadowing.

Rotary Shadowing

Isolated matrix proteins (10 to 20 μg/ml) were dissolved in 0.2 mol/L ammonium acetate in 50 to 70% glycerol, filled into a capillary, and sprayed onto freshly cleaved mica by a stream of N_2.[23] Mica chips were placed onto a rotary stage of a Balzers freeze-fracture unit (BAF 400 T, Balzers, Liechtenstein), dried at $<2 \times 10^{-5}$ mbar for 1 to 2 hours, and rotary shadowed with platinum at 7°C and carbon at 90°C. Replicas were floated in distilled water, picked up on 200-mesh glow discharged copper grids (Balzers CTA 010), and examined in a Jeol 1010 electron microscope.

SDS-PAGE and Immunoblotting

Soluble matrix proteins or intact matrix samples were solubilized by boiling for 3 minutes in reducing sample buffer (0.17 mol/L phosphoric acid, 0.31 mol/L Tris, 0.9 mmol/L EDTA-tetranatrium salt, 20% glycerol, 1% SDS, 36 mmol/L DTT), separated on 5 or 6% acrylamide gels, and stained with Coomassie Brilliant Blue G. Some gels were transferred onto nitrocellulose membranes and immunoblotted with the following antibodies: 1) rat monoclonal anti-laminin β1 IgG (1 to 2 μg/ml), 2) rat monoclonal anti-perlecan IgG (1 to 2 μg/ml), 3) rat monoclonal anti-entactin IgG (1 to 2 μg/ml), 4) rabbit anti-laminin-1 serum (~0.1 μg/ml), and 5) anti-EHS-collagen IV antiserum (~0.2 μg/ml). Immunoblots were developed by appropriate alkaline-phosphatase-labeled antibodies and chromogens.

Statistical Analysis

Experiments were performed in duplicate when not otherwise specified. Mean and standard deviations were calculated according to the F-test.

Results

Generation of ROS by the Fenton and Xanthine Oxidase/Xanthine Reactions

Pilot experiments were performed in the absence of EHS matrix to calibrate the production of ROS by the Fenton reaction by adjusting the amount of H_2O_2 added to Fe^{2+}. After addition of graded amounts of H_2O_2, the concentrations of the hydroxyl radical, a major product of the Fenton reaction, was monitored and found to correlate with the quantity of exogenous H_2O_2 added (Figure 1A). The complementary consumption of H_2O_2 in the Fenton reaction was monitored by iodometry (Figure 1B) and found to be initially relatively rapid (~4% within the first minutes), and to progressively slow down (~13% after 15 min-

utes and ~40% after 120 minutes). In controls without Fe^{2+}, no decay of H_2O_2 was observed.

Xanthine oxidase/xanthine was used as a continuous low-dose donor of H_2O_2 for the Fenton reaction in some experiments. The levels of H_2O_2 (<1 mmol/L) were at the threshold of sensitivity of direct iodometric quantitation, and therefore indirect determination by quantitation of superoxide anion by a sensitive enzymatic assay was performed (Figure 1C). This approach was valid because superoxide anion rapidly dismutates to provide H_2O_2.[18,24] Production of superoxide anion lasted for 60 minutes after initiation of the xanthine oxidase/xanthine reaction and generated a total of ~80 μmol of superoxide anion. In controls without xanthine, no enzymatic activity was detected.

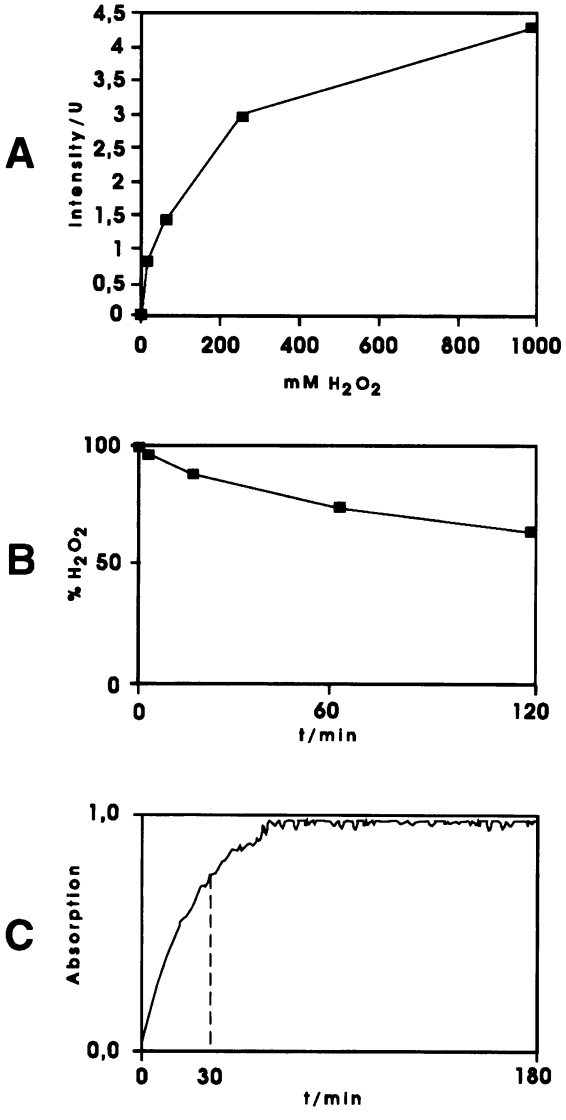

ROS Cause Partial Disassembly of EHS Matrix

Aliquots of suspended EHS matrix (8 mg ± 5%) were incubated with increasing concentrations of ROS produced by the Fenton reaction while keeping the incubation time constant at 120 minutes. In control incubations, PBS without ROS extracted ~200 μg/matrix aliquot, whereas TBS released ~60 μg, corresponding to 2.5 and 0.75% of the starting matrix protein; however, the relative percentages of protein released by ROS were similar in both buffers (Figure 2A). Low and intermediate concentrations of H_2O_2 (1 to 50 mmol/L) caused a dose-dependent release of proteins from EHS matrix, resulting in a mean maximal increase of ~480% when compared with controls without ROS (Figure 2A). This corresponded to solubilization of up to ~15% of the EHS matrix used for incubation. At higher concentrations of ROS (>50 mmol/L H_2O_2), less soluble protein was observed in the incubation media, presumably because of ROS-induced protein cross-linking and aggregation in the supernatants. In a second incubation protocol, concentrations of H_2O_2 (50 mmol/L) and Fe^{2+} were kept constant while incubation times were varied (0, 30, and 120 minutes). The amount of matrix proteins released from EHS matrix ranged from ~250% at 30 minutes to ~450% at 120 minutes when compared with controls (Figure 2B).

Figure 1. *Calibration and time course of ROS production in the absence of protein by the Fenton and the xanthine oxidase/xanthine reactions. The concentrations of hydroxyl radicals* (A), *the complementary H_2O_2 consumption during the Fenton reaction* (B), *and the generation of superoxide anion by xanthine oxidase/xanthine* (C) *are indicated. All experiments were performed in duplicate.* A: *The amount of hydroxyl radicals generated during incubation is controlled by H_2O_2 added to Fe^{2+} to initiate the Fenton reaction. Hydroxyl radicals were quantitated by fluorospectrometry to detect hydroxylated benzoate (excitation, 305 nm; emission, 407 nm). Increasing amounts of H_2O_2 were added to 0.5 mmol/L Fe^{2+} in 2 ml of TBS containing 200 μg of sodium benzoate and incubated for 15 minutes.* x *axis, final concentrations of H_2O_2 added;* y *axis, relative fluorescence intensity of hydroxylated benzoate as indicator of concentration of hydroxyl radicals. 1 U = 0.01 μg of quinine sulfate standard.* B: *Time course of H_2O_2 consumption by the Fenton reaction, complementary to generation of hydroxyl radicals. H_2O_2 was determined by iodometry. H_2O_2 (50 mmol/L) and Fe^{2+} (0.5 mmol/L) in TBS were incubated with 4 mmol/L methionine at 4°C, and 5-ml aliquots were drawn at different time points and were added to 15 ml of 0.2 N potassium iodite, 10 ml of 2 N H_2SO_4, and 5 ml of water. Back-titration was performed by 0.1 mol/L $Na_2S_2O_3$ with potato starch as indicator. In control experiments without Fe^{2+}, no decomposition of H_2O_2 was observed throughout the incubation time.* x *axis, incubation time;* y *axis, relative percentage of H_2O_2, as compared with the starting concentration.* C: *Time course of superoxide anion production by xanthine oxidase/xanthine, as indirect indicator of H_2O_2 generation. Superoxide anion was measured by a kinetic photometric assay for the conversion of xanthine to urate by xanthine oxidase (3 mU/ml)/xanthine (1.2 mmol/L) with 0.3 mmol/L Fe^{2+} and 0.1 mmol/L EDTA in PBS (final volume, 1 ml) and expressed as increase in absorption at 295 nm, $\Delta\epsilon = 1.24 \times 10^4$ mol/L^{-1} cm^{-1}. In total, 80 μmol of superoxide anion were produced. In controls without xanthine, no enzymatic activity was detected. One unit is defined as 1 μmol of urate/minute.* x *axis, incubation time;* y *axis, absorption at 295 nm.*

EHS matrix was also incubated with continuously produced low doses of ROS produced by the xanthine oxidase/xanthine reaction. After 30 minutes of incubation, ~570%, and after 120 minutes, ~690% of matrix proteins were liberated when compared with controls (Figure 2C). This corresponded to ~17% of protein of the starting matrix. Additional control incubations were performed with xanthine oxidase without xanthine, which excluded the possibility that degradation by contaminating proteases was a cause of protein release from the EHS matrix (Figure 2C).

These results indicate that treatment of assembled intact EHS matrix with ROS resulted in partial dissociation of matrix and release of matrix proteins into the incubation media.

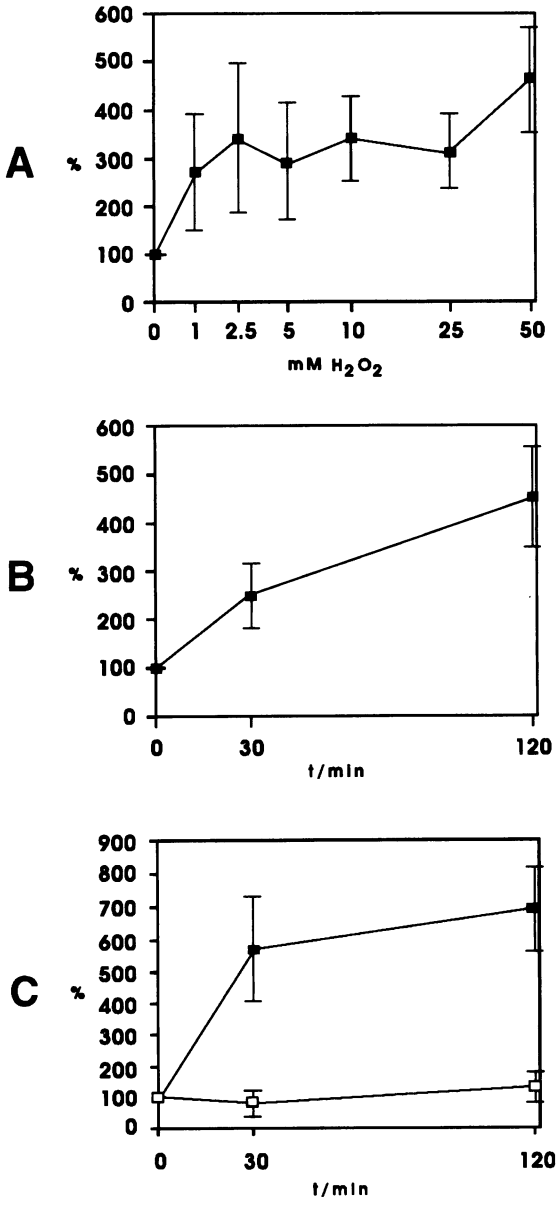

ROS Induce Cross-Linking of EHS Matrix

While ROS extracted ~15% of protein from the EHS matrix, the residual EHS matrix remained undissociated. This could be due to cross-links present already in the starting EHS matrix and/or additional ROS-induced cross-linking, eg, by formation of bityrosine residues. As indicator for this possibility, the amount of matrix protein released by EDTA (predominantly laminin) was determined from EHS matrices after control and ROS-containing incubations. EDTA buffer extracted approximately three times more protein in controls than from ROS-incubated residual matrix (values corrected for laminin released by ROS in the preceding step; Figure 3), suggesting that laminin and presumably also other matrix proteins were cross-linked by ROS. Adduct formation by lipid peroxidation products, another potential cross-linking mechanism, was not encountered.

Laminin Is Released from EHS Matrix at Lower ROS Concentrations than Type IV Collagen

Matrix proteins released from the EHS matrix into the incubation media by graded concentrations of ROS were analyzed by rotary shadowing and electron microscopy. Monomeric laminin (~80% complexed with entactin, data not shown) was found in control incubations without ROS. Also at low concentrations

Figure 2. *ROS partially disassemble EHS matrix and release matrix proteins into the incubation media. Experiments were performed in triplicate; vertical bars are the standard deviations.* **A:** *Dose-response relationship of release of EHS matrix proteins by increasing concentrations of ROS produced by the Fenton reaction. Aliquots of 8 mg ± 5% EHS matrix were suspended in buffer containing 0.3 mmol/L Fe^{2+} and incubated with increasing concentrations of H_2O_2 for 120 minutes at 4°C. Protein concentrations were determined by the Coomassie Plus assay.* x *axis, final concentrations of H_2O_2 added to the incubation buffers, expressed in ln(x + e) to accommodate a wide range of concentrations;* y *axis, protein released by ROS, expressed as percentage of protein released when incubated without H_2O_2 (100%).* **B:** *Time-response relationship of protein release from EHS matrix into the incubation media by ROS produced by the Fenton reaction. Aliquots of 8 mg ± 5% EHS matrix were suspended in buffer containing 0.3 mmol/L Fe^{2+} and were incubated with 50 mmol/L H_2O_2 for 30 and 120 minutes.* x *axis, incubation times;* y *axis, protein released by ROS, expressed as percentage of protein released when incubated in buffer without H_2O_2 (100%).* **C:** *Time-response relationship of protein released from assembled EHS matrix into the incubation media by ROS produced by the xanthine oxidase reaction (■). Aliquots of 8 mg ± 5% EHS matrix were suspended in buffer containing 0.3 mmol/L Fe^{2+} and 0.1 mmol/L EDTA and were incubated with constant amounts of xanthine oxidase (3 mU) and xanthine (1.2 mmol/L) for 30 and 120 minutes. In controls, xanthine was omitted (□).* x *axis, incubation time;* y *axis, protein released by ROS, expressed as percentage of protein released when incubated in buffer without xanthine oxidase and xanthine (100%).*

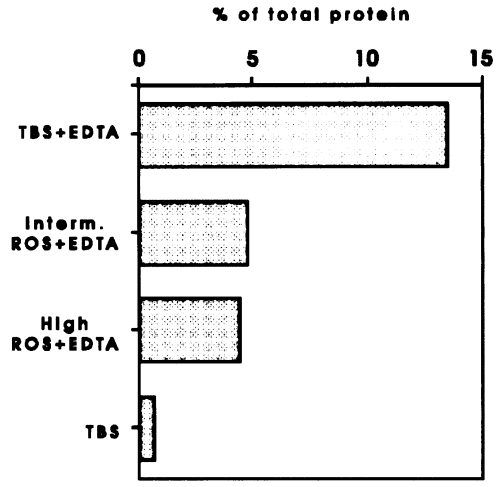

Figure 3. *Disintegration of EHS matrix by EDTA is partially inhibited by ROS-mediated cross-linking. When aliquots of EHS matrix were incubated in 20 mmol/L EDTA in TBS for 60 minutes at 20°C, ~14% of total protein was released in soluble form (TBS + EDTA). When, however, EHS matrix was incubated first with intermediate or high ROS concentrations (20 or 150 mmol/L H_2O_2, 0.3 mmol/L Fe^{2+}; 120 minutes at 4°C) and then extracted with 20 mmol/L EDTA, only <5% of total protein was released (Interm. and High ROS + EDTA). TBS without EDTA extracted <1% EHS matrix protein (TBS). x axis, protein released by 20 mmol/L EDTA, expressed as percentage of total EHS protein, corrected for laminin released by preceding ROS incubation. Values are means of a duplicate determination.*

of ROS (induced by 1 to 10 mmol/L H_2O_2), morphologically intact laminin was observed (~60% complexed with entactin; Figure 4, A and B). At intermediate ROS concentrations (induced by 50 mmol/L H_2O_2), damaged laminin was observed that was devoid of entactin and that showed various degrees of structural damage, ranging from distortion of its cross shape to loss of peripheral globular domains and entire arms (Figure 4C). In addition, few type IV collagen molecules were found in these preparations. At high ROS concentrations (induced by 150 mmol/L H_2O_2), only heavily fragmented laminin and small globular proteins were observed. Type IV collagen dominated in these preparations, frequently as dimers and oligomers lacking the lateral 7 S domains (Figure 4D). In addition, large aggregates of matrix proteins were observed in which fragments or components of laminin or collagen were occasionally recognized (Figure 4, E and F). Intriguingly, proteoglycans were never found in the supernatants. Similar results were obtained in both incubation protocols of the Fenton reaction, ie, variation of external H_2O_2 or variation of incubation times at constant H_2O_2 concentration. In the xanthine oxidase/xanthine reaction, only soluble intact laminin/entactin complexes were observed (data not shown), consistent with the results described above for low concentrations of ROS directly produced by the Fenton reaction.

Proteins released by ROS into the incubation media were identified by SDS-PAGE and Coomassie Blue staining and by immunoblotting with matrix protein-specific antibodies. The same proteins were observed in controls and at low concentrations of ROS (Figure 5, lanes A to C), including laminin $\beta1/\gamma1$ and $\alpha1$ chains with apparent molecular weights (MWs) of ~200 and ~400 kd (Figure 5, lane D) and entactin with apparent MW of ~158 kd (Figure 5, lane E). At low concentrations of ROS, also oligomeric aggregates were observed at the top of the resolving gels (Figure 5, lanes B and C). At intermediate ROS concentrations (Figure 5, lane G), essentially the same protein pattern was found. At high concentrations of ROS, two type IV collagen chains with apparent MWs of ~180 and ~165 kd became prominent (Figure 5, lanes H to J) whereas laminin and entactin were decreased. Anti-perlecan IgG failed to detect any band in the supernatant at any concentration of ROS (Figure 5, lanes F and K).

When the residual matrix after incubation with ROS was extracted with reducing SDS sample buffer and analyzed by SDS-PAGE and immunoblotting, similar protein patterns were found as in matrix incubated with buffer in the absence of ROS (data not shown). Perlecan was detected at the top of the gels, and chains of laminin, entactin, and type IV collagen were intact. However, solubilization of matrix samples in reducing SDS sample buffer was variable and incomplete.

Isolated EHS Matrix Proteins Show Graded Sensitivity to ROS

Incubation of soluble EHS matrix proteins with increasing concentrations of ROS yielded a more precise and detailed inventory of morphological changes of individual matrix proteins (Figure 6). In control incubations, aliquots of matrix protein were incubated in buffer without H_2O_2 and analyzed by rotary shadowing (Figure 6A). They consisted of >90% monomeric laminin, ~50% of which was associated with entactin (Figure 6, B–D), as well as a few laminin dimers (Figure 6E). Type IV collagen constituted <3% of all molecules. Unspecified globular and dumbbell-shaped proteins of ~10 nm diameter were infrequently encountered. Proteoglycans were not identified. Increasing concentrations of ROS induced variable forms of damage of laminin, ranging from detachment of entactin to distortion of arms, loss of peripheral domains, progressive mutilation of laminin crosses, and complete degradation (Figure 6, G–M). By contrast, type IV collagen re-

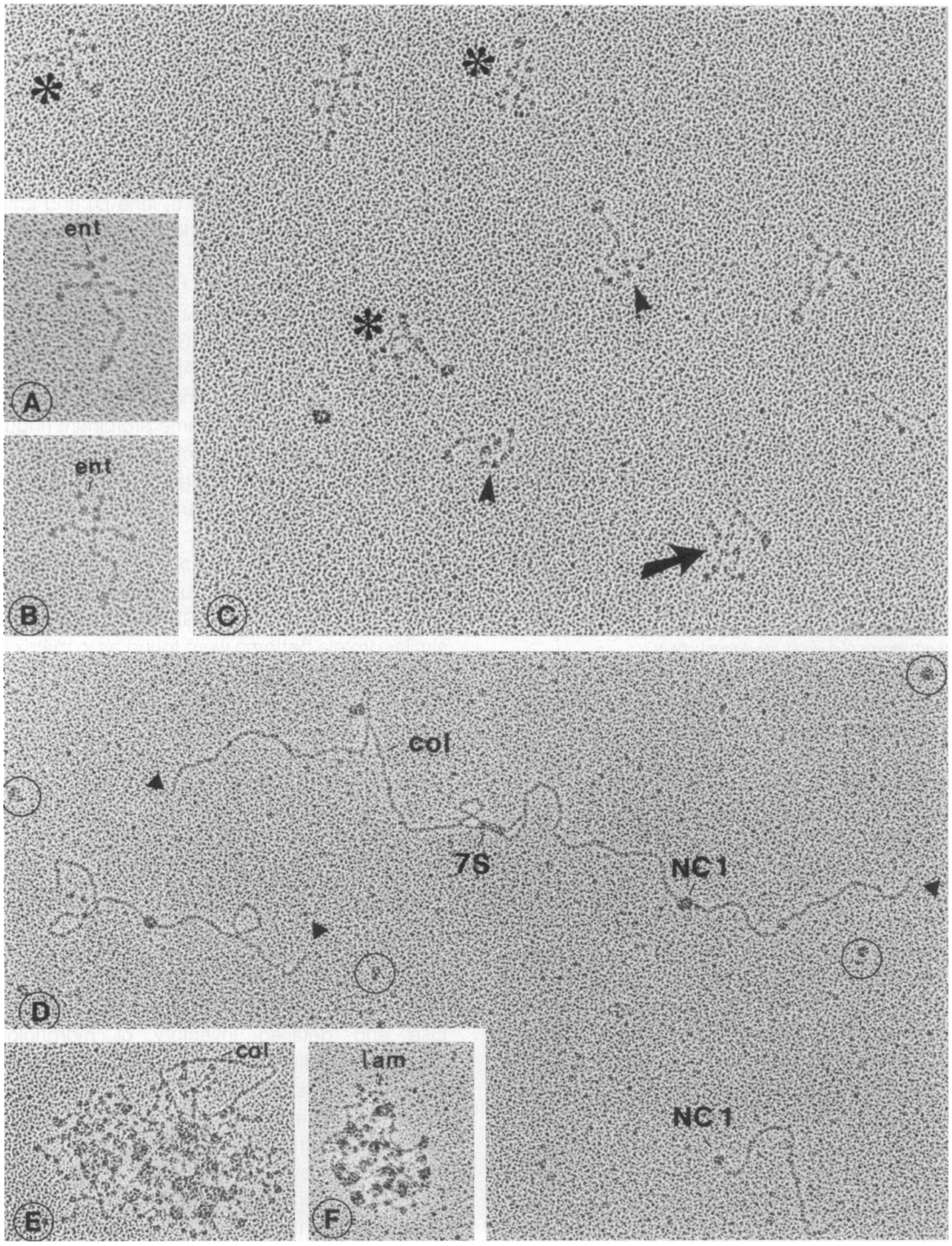

Figure 4. *Laminin is released from EHS matrix at lower concentrations of ROS than type IV collagen, as seen by rotary shadowing. Gallery of representative views of matrix proteins released into the incubation media from EHS matrix at low* (A *and* B), *intermediate* (C), *and high* (D *to* F) *concentrations of ROS.* A *and* B: *Regular shaped laminin/entactin* (*ent*) *complexes released at low ROS concentrations* (*induced by 2.5 mmol/L* H_2O_2, *0.3 mmol/L* Fe^{2+}; *120 minutes at 4°C*) *identical with those released in control incubations without ROS.* C: *Laminin released at intermediate concentrations of ROS* (*induced by 75 mmol/L* H_2O_2, *0.3 mmol/L* Fe^{2+}; *120 minutes at 4°C*), *showing a spectrum of damage, ranging from loss of entactin* (arrows) *to massive twisting of the cross shape* (asterisks) *to loss of peripheral globular domains and whole arms* (arrowheads). D: *At a higher ROS concentration* (*induced by 150 mmol/L* H_2O_2, *0.3 mmol/L* Fe^{2+}; *120 minutes at 4°C*), *the predominant protein was type IV collagen* (*col*), *preferentially in oligomers that laterally lack 7 S domains* (▲). *Fragmented laminin was occasionally found, whereas intact laminin was absent. Unspecified globular proteins are indicated by* circles. E *and* F: *Oligomeric aggregates* (*aggr*) *are formed at high concentrations of ROS. Remnants of laminin* (*lam*) *and type IV collagen* (*col*) *were identified. Magnification,* ×140,000.

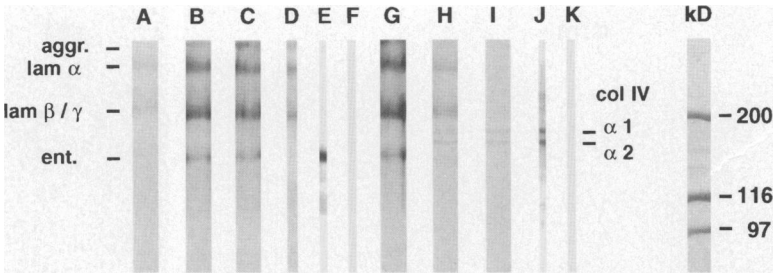

Figure 5. *Identification of matrix proteins released at different concentrations of ROS into the incubation media. Proteins were separated by 5% SDS-PAGE and stained with Coomassie Blue* (lanes A *to* C *and* G *to* I) *or immunoblotted with matrix protein-specific antibodies* (lanes D *to* F, J, *and* K). *The experiment was performed in triplicate.* Lanes A *to* E: *At lower ROS concentrations, proteins with apparent MWs of 158, ~200, and ~400 kd* (lane A, *control;* lane B, *ROS induced with 2.5 mmol/L H_2O_2;* lane C, *10 mmol/L H_2O_2) were released, which are identified by immunoblotting* (lanes D *and* E) *as entactin (158 kd), laminin β1/γ1 (200 kd), and laminin α1 (400 kd).* Lane F *shows that perlecan is not detected by immunoblotting.* Lanes G *to* K: *Intermediate and high concentrations of ROS in the incubation media release also laminin and entactin, similar to lower concentrations of ROS* (lane G, *ROS induced with 50 mmol/L H_2O_2). Maximal protein release is observed at 50 mmol/L H_2O_2* (lane G). *With increasing levels of ROS, these bands fade away and two proteins with apparent MWs of 165 and 180 kd become prominent* (lane H, *ROS induced by 75 mmol/L H_2O_2;* lane I, *150 mmol/L H_2O_2) that are type IV collagen α1 and α2 chains* (lane J). *Perlecan is not detected even at high concentrations of ROS* (lane K). *Oligomeric aggregates consisting primarily of laminin are detected at the top of the gels* (lanes B, C, *and* G). *MWs are indicated by globular protein standards.*

mained apparently unfragmented, even at high ROS concentrations, and therefore appeared relatively enriched (Figure 6, K and L). Aggregates became prominent at high ROS concentrations (Figure 6N).

Equal aliquots of matrix proteins incubated with ROS or with control buffer were analyzed by SDS-PAGE (Figure 7, A and B) and immunoblotting. An inventory of proteins of the control matrix comprised the ~200- and ~400-kd laminin β1/γ1 and α1 chains and 100- and 105-kd fragments of entactin (Figure 7, lane A). A >600-kd band on the top of the resolving gels corresponded to <5% of total protein and was labeled by anti-laminin IgG. The ~185-, ~200-, and ~380-kd proteins were poorly stained by Coomassie Blue and were identified as α1, α2 chains and dimers of type IV collagen (Figure 8, lane 1). Incubation with low ROS concentrations caused rapid and almost complete degradation of the entactin fragments (Figure 7, lane B). With increasing ROS concentrations, laminin chains progressively disappeared, with a more pronounced loss of the β1 and γ1 chains than of the α1 chains (Figure 7, lanes B to F). In addition, the β1 and γ1 chains showed a slightly increased electrophoretic mobility. The patterns of type IV collagen α1, α2 chains and dimers remained unchanged at low and intermediate ROS concentrations and abruptly changed into a broad streak at high ROS concentrations (Figure 8, lanes A to F).

Low Concentrations of ROS Cause Oxidation of Tryptophan Residues in Laminin

Laminin released from intact EHS matrix at very low concentrations of ROS (induced by 2.5 mmol/L H_2O_2) showed ~50% reduction of tryptophan-specific fluorescence, indicating damage of this particularly oxidation-sensitive amino acid. When small amounts of ROS (induced by 0.5 and 1 mmol/L H_2O_2) were incubated with soluble matrix protein fractions containing primarily laminin, rapid and almost complete loss of tryptophan-specific fluorescence was observed, whereas Fe^{2+} or H_2O_2 separately showed only minimal reduction (Figure 9, A and B). This indicated that tryptophans of laminin were damaged by low concentrations of ROS, at which morphological damage was absent.

ROS-Modified Laminin Fails to Polymerize

Spontaneous homotypic association of intact laminin (1.4 mg/ml TBS) was achieved by incubation for 130 minutes at 37°C (Table I). The pelleted polymer could be subsequently redissolved in 20 mmol/L EDTA in TBS. By contrast, laminin incubated with very low concentrations of ROS (induced by 0.5 mmol/L H_2O_2) failed to associate under these conditions. Although its morphology appeared intact, >70% of its tryptophans were damaged by oxidation. At higher concentrations of ROS (induced by 20 mmol/L H_2O_2), laminin formed covalent aggregates, which, however, failed to dissolve in 20 mmol/L EDTA and also 5 mmol/L DTT.

Aggregate Formation Correlates with Oxidative Dimerization of Tyrosine Residues

With increasing concentrations of ROS covalently linked, nonreducible oligomeric aggregates of laminin and type IV collagen were formed from soluble matrix proteins (Figure 10). When the formation of

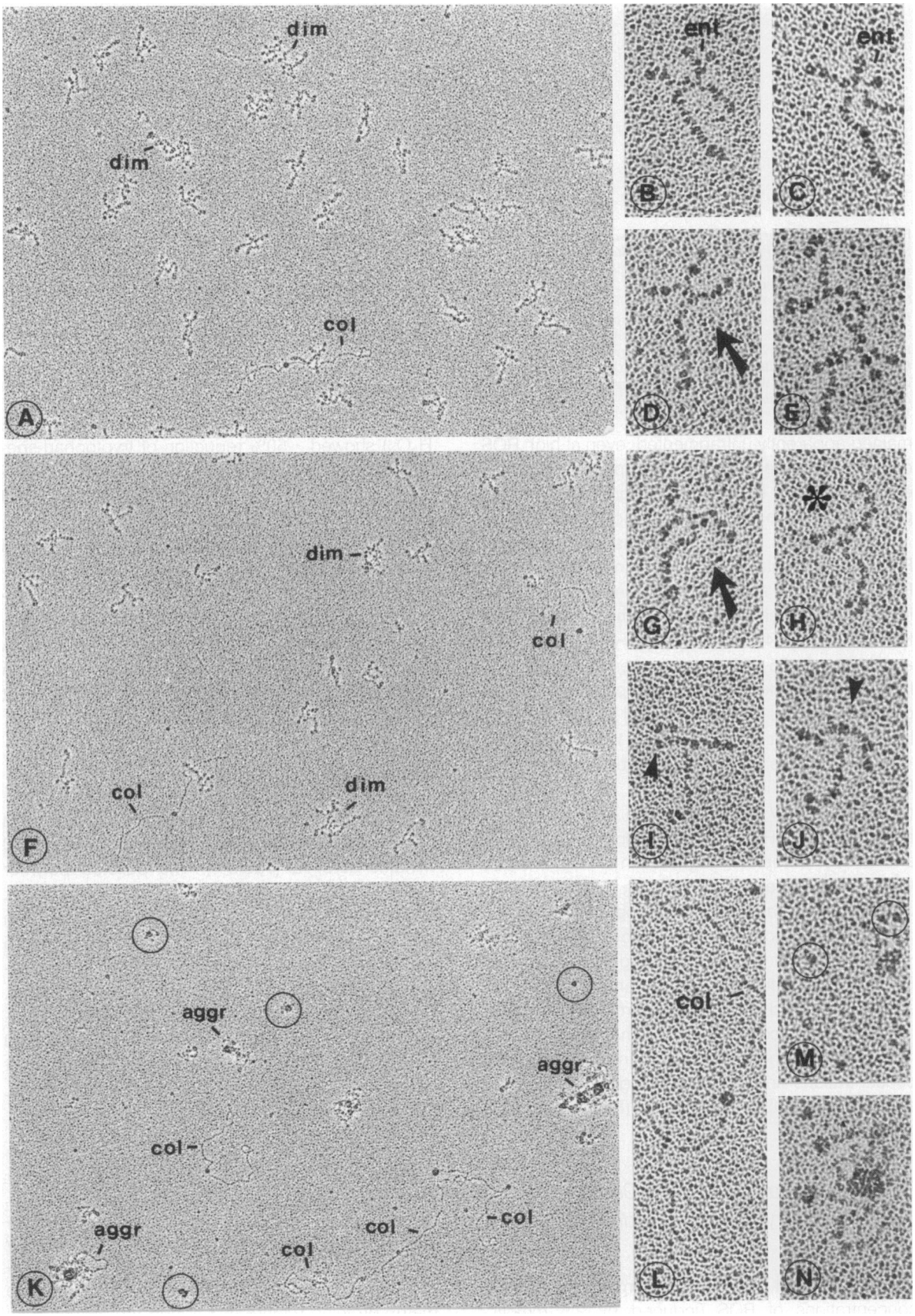
dim
dim
col
A
ent
B
ent
C
D
E
dim
col
col
dim
F
G
H
I
J
aggr
aggr
col
aggr
col
col
col
K
col
L
M
N

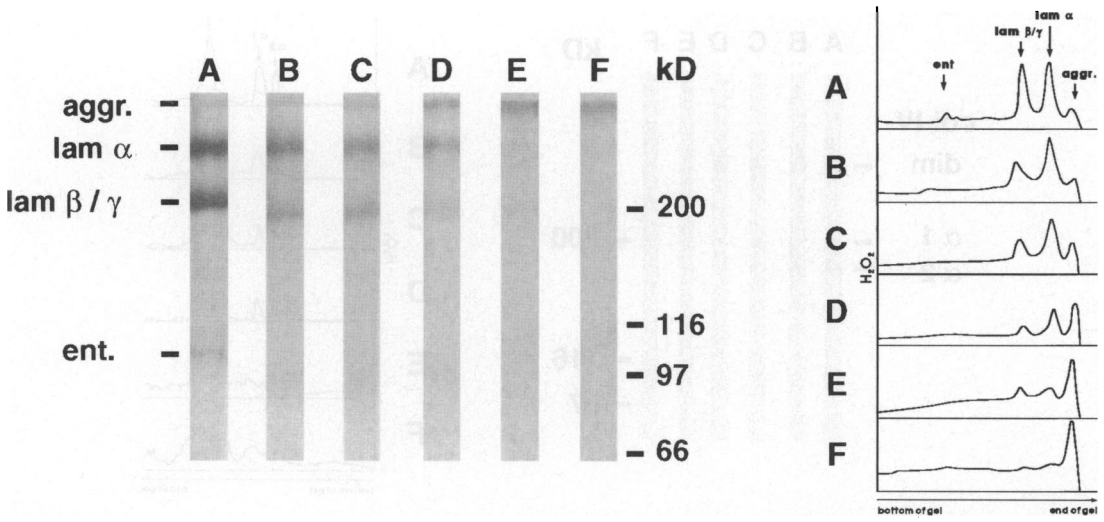

Figure 7. *Dose-response relation of concentration of ROS in the incubation media and degradation and aggregation of matrix proteins. Equal aliquots of soluble isolated EHS matrix proteins were incubated in TBS with 0.5 mmol/L Fe^{2+} for 15 minutes at 4°C with increasing concentrations of ROS, induced by the Fenton reaction at H_2O_2 concentrations of 0 mmol/L (control;* A*), 30 mmol/L (*B*), 60 mmol/L (*C*), 180 mmol/L (*D*), 600 mmol/L (*E*), and 1200 mmol/L (*F*). The experiment was performed four times.* Left: *Polyacrylamide gel (5%) stained with Coomassie Blue onto which equal aliquots of ROS-incubated matrix proteins were loaded. With increasing ROS concentrations, entactin and laminin chains progressively disappear in the sequence entactin > laminin β1/γ1 > laminin α1, whereas aggregates are building up.* Right: *Quantitative evaluation by laser densitometry, showing the kinetics of decay of entactin and laminin and the countercurrent formation of covalent oligomeric aggregates.*

bityrosines, an established ROS-mediated cross-linking reaction,[14] was determined, a direct correlation with ROS concentration and aggregate formation was found (Figure 10). High concentrations of H_2O_2 (1200 mmol/L) alone without Fe^{2+} and in the presence of deferoxamine yielded 50 to 70% bityrosines of those produced by the Fenton reaction. Thiobarbituric-acid-reactive substances, such as the cross-linking lipid peroxidation adducts malone dialdehyde and 4-hydroxynonenal were not detected (data not shown).

Degradation of Laminin and Entactin Is Caused Primarily by Hydroxyl Radicals

Definition of the ROS compounds responsible for matrix protein damage was achieved by use of the ROS scavengers DMTU, methionine, catalase, superoxide dismutase, and deferoxamine (Figure 11), which are known to interfere with unique reactive products and intermediates of the Fenton reaction. Fractions of soluble matrix proteins were incubated at constant high concentration of ROS (induced by 1200 mmol/L H_2O_2), ie, conditions at which >95% of entactin and laminin chains were destroyed in the absence of scavengers (Figure 11, lane B). Degradation of laminin and entactin was significantly inhibited by the hydroxyl radical scavengers DMTU (Figure 11, lane C) and less effectively by methionine (Figure 11, lane D). Deferoxamine (Figure 11, lane G) and catalase (Figure 11, lane E) prevented formation of the hydroxyl radical and reduced degradation of matrix proteins. The superoxide anion scavenger superoxide dismutase (Figure 11, lane F) almost completely failed to inhibit protein degradation. Taken together, these findings suggest that the hydroxyl radical was the main species responsible for matrix protein degradation.

Formation of oligomers and aggregates was apparently induced not only by hydroxyl radicals but also by H_2O_2 alone, because they were not prevented by deferoxamine (Figure 11, lane G), whereas DMTU (Figure 11, lane C), which scavenges hydroxyl radicals and H_2O_2, completely inhibited their formation. This finding was confirmed by rotary shadowing of matrix proteins incubated with

Figure 6. *Gallery of morphological alterations of isolated, soluble EHS matrix proteins incubated with increasing concentrations of ROS.* A *to* E: *Soluble isolated matrix proteins were incubated in buffer without ROS. Monomeric and occasionally also dimeric (dim) laminin is observed, with ~50% of laminin forming complexes with entactin (ent;* B *to* D*). Type IV collagen dimers are minor constituents.* F *to* J: *At intermediate concentrations of ROS (induced by 30 to 180 mmol/L H_2O_2, 0.5 mmol/L Fe^{2+}; incubation for 15 minutes at 4°C), detachment of entactin (*arrows, G*) and distortion of arms (*asterisks, H*) are frequently found. With increasing ROS concentrations, loss of peripheral domains (*I*) or of arms (*arrowheads, J*) are encountered. Type IV collagen dimers and monomers (col) show regular shapes (*F*).* K *to* N: *High concentrations of ROS (induced by 1200 mmol/L H_2O_2) cause complete loss of laminin and entactin. Type IV collagen dimers and less frequently monomers predominate (*K*. Unspecified globular proteins (*M, circles*) and aggregates (aggr;* K *and* N*) are prominent. Magnification, ×75,000 (*A, F, *and* K*) and ×230,000 (*B *to* E, G *to* J, *and* L *to* N*).*

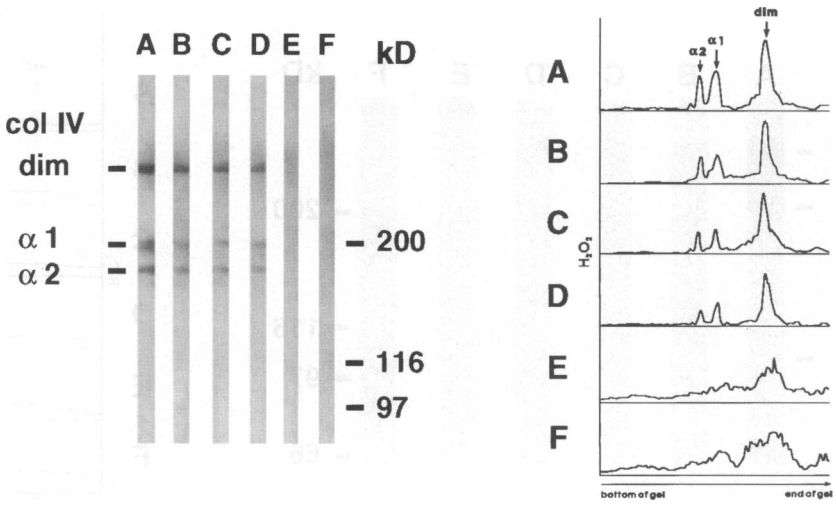

Figure 8. *Effects of ROS on soluble, isolated type IV collagen. Equal aliquots of soluble isolated EHS matrix proteins were incubated in TBS with 0.5 mmol/L Fe^{2+} for 15 minutes at 4°C with increasing concentrations of ROS, induced by the Fenton reaction at H_2O_2 concentrations of 0 mmol/L (control;* **A**), *30 mmol/L* (**B**), *60 mmol/L* (**C**), *180 mmol/L* (**D**), *600 mmol/L* (**E**), *and 1200 mmol/L* (**F**). *After separation by SDS-PAGE and transfer onto nitrocellulose, immunoblotting with anti-type IV collagen antibodies for each strip under identical conditions was performed. The experiment was performed four times.* Left: *Immunoblotting with anti-type-IV-collagen antibodies. Type IV collagen α1 and α2 chain monomers and dimers remained intact up to a ROS concentration induced by 600 mmol/L H_2O_2* (**E**), *at which the sharp bands converted into broad streaks* (**E** *and* **F**). Right: *Quantitative evaluation by laser densitometry, showing relative resistance of collagen chains to ROS up to 600 mmol/L H_2O_2.*

H_2O_2 and deferoxamine, which showed increased numbers of intact laminin oligomers (data not shown).

Role of Metalloproteases in ROS-Induced Degradation of Matrix Proteins

Metalloproteases are frequently associated with matrix proteins, especially with laminin,[25] and are activated by ROS.[26] Thus, it was relevant to assess their potential contribution to the degradation of matrix proteins and to distinguish their action from that of ROS. When the metal ion chelator 1,10-phenanthroline was included as a metalloprotease inhibitor into incubation media, only minimal reduction of the degradative effects of ROS was observed (Figure 11H). This suggested indirectly that degradation of matrix proteins was primarily due to ROS.

Discussion

Infiltration of tissues by inflammatory and tumor cells requires cell migration through the complex glycoprotein meshworks of intercellular matrix and basement membranes. Although roles of proteases for focal degradation of matrix are established, the contributions of ROS produced especially by activated cells[27–31] were not analyzed in detail. ROS cause several chemical protein modifications, such as cleavage of peptide bonds, formation of cross-links, and oxidation of aromatic and other amino acid residues.[14,32,33] Because of the complex structures of natural matrices, it was technically difficult to identify specific ROS-induced damage on individual matrix proteins and to assess consequences for matrix assembly and dissociation *in vivo*. We have chosen to analyze *in vitro* the actions of ROS on the EHS sarcoma matrix that consists primarily of laminin, entactin, type IV collagen, and the heparan sulfate proteoglycan perlecan.[12,19] These matrix proteins assemble in a three-dimensional meshwork, composed by two largely independent homopolymeric networks of laminin and type IV collagen[22] that are connected via entactin and perlecan bridges.[3] EHS matrix differs, however, in several aspects from natural basement membranes, such as the GBM, in that the subspecies of laminin and type IV collagen are different. Specifically, the EHS matrix contains laminin 1 and $\alpha 1_2/\alpha 2$ type IV collagen, whereas laminin 3 (S-laminin) and $\alpha 3_2/\alpha 4$ type IV collagen predominate in the GBM. Moreover, it is not known whether the two-polymer model of EHS matrix also applies to basement membranes.

In this study, assembled EHS matrix, or fractions of isolated soluble EHS matrix proteins were incubated *in vitro* with precisely adjusted concentrations of ROS produced by the Fenton or the xanthine oxidase/xanthine reactions. These ROS-generating systems also occur *in vivo* and provide a wide spectrum of ROS, such as hydroxyl radicals, H_2O_2, and superoxide anion.[34–37] Matrix proteins were examined for oxidative damage by rotary shadowing,

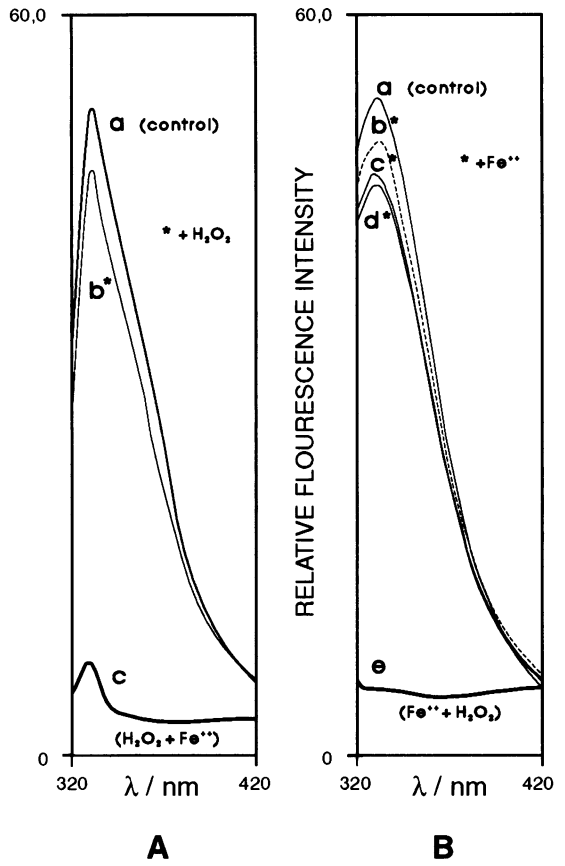

Figure 9. *Loss of tryptophan-specific fluorescence (excitation, 280 nm; emission scan, 320 to 420 nm) in ROS-induced oxidative damage of laminin/entactin. The experiment was performed in duplicate with the same result.* A: *To an aliquot of a laminin- and entactin-enriched matrix protein fraction in TBS* (a), *in a first step,* H_2O_2 *(final concentration, 0.5 mmol/L;* b), *and in a second step,* Fe^{2+} *(final concentration, 0.3 mmol/L;* c) *were added.* H_2O_2 *alone causes only slight reduction of tryptophan fluorescence* (b), *whereas* Fe^{2+}*-induced ROS production results in massive decrease* (c). B: *To an equal aliquot of a laminin- and entactin-enriched matrix protein fraction in TBS* (a), Fe^{2+} *(0.3 mmol/L) was added, followed by triplicate determination of fluorescence in intervals of 2 minutes* (b *to* d) *and by addition of 1 mmol/L* H_2O_2 (c). *Also in this setting, rapid and almost complete loss of tryptophan-specific fluorescence is found when both Fenton reactants were added.* x *axis, wavelength of emission ranging from 320 to 420 nm;* y *axis, relative fluorescence intensity, with 1 U equivalent to a standard of 0.01 μg of quinine sulfate.*

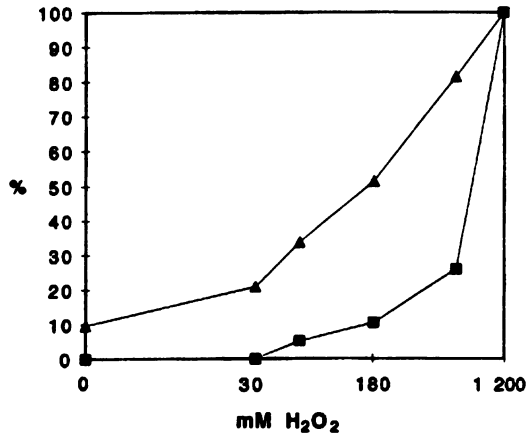

Figure 10. *ROS-induced formation of oligomeric matrix protein aggregates (▲) and bityrosine residues (■) follows a dose-effect relation. Aggregates were quantitated from SDS gels by densitometry, and bityrosine residues were quantitated by fluorospectrometry at excitation at 325 and emission at 415 nm. Increasing concentrations of ROS were produced by adding* H_2O_2 *(0 to 1200 mmol/L) to TBS with 0.5 mmol/L* Fe^{2+} *and incubating for 15 minutes at 4°C.* x *axis,* H_2O_2 *concentration expressed in ln(x + e) to accommodate a wide range of concentrations;* y *axis, percentage of oligomers or bityrosines expressed as percentage of those obtained by the highest ROS concentration produced by 1200 mmol/L* H_2O_2*. Values are means of a duplicate determination.*

quantitative SDS-PAGE, and immunoblotting and by fluorospectrometry to detect oxidative damage of tryptophan residues and formation of bityrosine links

A major finding of this investigation was that ROS partially disintegrate EHS matrix in a dose-dependent fashion. Up to ~15% of matrix proteins were released in soluble form, corresponding to up to seven times that obtained in control incubations without ROS. This raised questions as to the selectivity of damage for distinct matrix proteins and the type and extent of oxidative damage of matrix proteins set free into the incubation media.

Laminin and laminin/entactin complexes were selectively released into the incubation medium at relatively low concentrations of ROS. Although the morphology and chain sizes of the complexes appeared

Table 1. *Inhibition of Homotypic Polymerization of Laminin by Low Concentrations of ROS and Formation of Covalent Cross-Links at Intermediate Concentrations of ROS*

H_2O_2 added	Laminin polymerized/ aggregated	Fluorescence of tryptophans	Pellet dissolved by EDTA	Laminin shape
Control	30%	100%	100%	Intact
0.5 mmol/L	<1%	29%		Intact
20 mmol/L	37%	<5%	<1%	Damaged

1.4 mg/ml aliquots of isolated EHS matrix protein fractions enriched for laminin (>95%) were incubated for 130 minutes at 37°C without, or with very low (0.5 mM H_2O_2, 0.5 mM Fe^{2+}), or intermediate concentrations (20 mM H_2O_2, 0.5 mM Fe^{2+}) of ROS. The amount of polymerized or aggregated proteins was expressed as the percentage of the starting protein concentration. Insoluble protein polymers were pelleted and dissolved in 20 mM EDTA in TBS. Whereas polymers formed in control incubations without ROS are EDTA-soluble, small amounts of ROS efficiently inhibit laminin assembly. Whereas at these ROS concentrations the shape of laminin was intact, extensive oxidative damage of tryptophan residues was observed. By contrast, aggregates formed by high ROS concentrations were insoluble in EDTA, presumably because of covalent ROS-induced cross-linking. At this ROS concentration laminin morphology was damaged, and tryptophan-specific fluorescence was almost completely abolished.

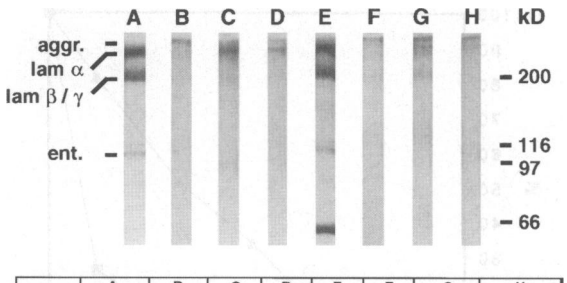

Protein	A Starting Material	B ROS Control	C ROS + DMTU	D ROS + Met	E ROS + Catal.	F ROS + SOD	G ROS + Deferox.	H ROS + Phenanthr.
Lam α	100%	5%	68%	23%	100%	9%	39%	20%
Lam β/γ	100%	2%	26%	0%	100%	0%	35%	0%
Ent.	100%	0%	0%	0%	100%	0%	0%	0%
Aggr.	5%	100%	5%	61%	5%	89%	120%	92%

Figure 11. *Identification of the hydroxyl radical as the major species responsible for degradation of matrix proteins and the role of degradative activity of metalloproteases. Soluble isolated EHS matrix proteins were incubated with high concentrations of ROS (induced by 1200 mmol/L H_2O_2 and 0.5 mmol/L Fe^{2+}; 15 minutes at 4°C), with several ROS scavengers* (B *to* G) *and a metalloprotease inhibitor* (H), *and subjected to SDS-PAGE* (upper panel) *and laser densitometry* (lower panel) *for quantitative evaluation. The composition of the untreated soluble matrix protein fraction is shown in* A. Lane B *and* column B *show almost complete oxidative degradation of matrix proteins and simultaneous formation of aggregates by ROS. In* C, *degradation and aggregation are effectively inhibited by DMTU (168 mmol/L). Significant inhibition of degradation and aggregation is also obtained with methionine (37 mmol/L) in* D *and with deferoxamine mesylate (75 μmol/L) in* G. *Complete inhibition of degradation and aggregation is achieved with catalase (11,500 U/ml) in* E, *with the strong band at ~60 kd, indicating the enzyme. Superoxide dismutase (1600 U/ml) in* F *has almost no effect in preventing ROS-mediated degradation/aggregation.* Lane H *and* column H *show that metal ion chelating by 1,10-phenanthroline (1 mmol/L) has almost no influence in ROS-induced degradation/aggregation. The experiment was performed in duplicate.*

intact by rotary shadowing and SDS-PAGE, extensive oxidative damage of tryptophans was observed. Intriguingly, this soluble oxidized laminin failed to associate to form polymers, suggesting irreversible intramolecular conformational changes, similar to those observed in laminin by *in vitro* glucosylation.[38] By analogy, low-dose ROS-induced changes of molecular conformation without gross molecular damage were recently found to cause complete loss of enzymatic activity of acetyl cholinesterase.[39] With increasing concentrations of ROS in the incubation media, gradual mutilation of laminin molecules was observed, ranging from apparent loss of its rigid cross shape and random detachment of individual globular units and arms to complete fragmentation and disassembly. In SDS gels, these morphological changes were paralleled by progressive loss of individual laminin chains, with the 200-kd chains being apparently more sensitive than the 400-kd chain.

Entactin in the laminin/entactin complexes was found to be the most ROS-sensitive matrix protein. It remains to be determined whether ROS-induced release of laminin is influenced by damage of entactin that mediates heterotypic laminin-collagen contacts and stabilizes EHS matrix.[3]

The type IV collagen network in the EHS matrix was more resistant to ROS than laminin. Collagen was released from intact EHS matrix at high concentrations of ROS, at which entactin and laminin were already severely damaged or completely degraded. Most of the released type IV collagen formed dimers or oligomers, lacking the amino-terminal linkage forming 7 S regions of the lateral edges. This could explain why small oligomeric groups of type IV collagen were detached from homotypic associations in the matrix. Experiments with soluble isolated type IV collagen indicated that up to relatively high concentrations of ROS collagen chains migrated in sharp bands that changed abruptly at 600 mmol/L H_20_2 to broad streaks. Simple explanations could be partial fragmentation and aggregation of type IV collagen or alterations in molecular shape and rigidity that were not apparent by rotary shadowing. Degradation of type IV collagen occurred at higher concentrations of ROS than of type I collagen.[40]

Perlecan was not detected by biochemical or morphological methods in the supernatant at any ROS concentration used. However, intact perlecan remained within the ROS-treated matrix, even when laminin and type IV collagen were partially solubilized, suggesting that perlecan was not released by ROS or that a small fraction was released and rapidly degraded. This is in agreement with the observation that perfusion of kidneys with xanthine oxidase and xanthine failed to degrade GBM proteoglycans, whereas their concentration in the GBM and in the perfusion media decreased.[41] The apparent resistance of the perlecan core protein to ROS is, however, in contrast to chondrocyte proteoglycans, in which massive degradation was induced by similar concentrations of ROS as used in this study.[42] This could be due to different chemical structures and/or accessibility of proteoglycans in cartilage. Oxidative derivatizations and fragmentations of EHS-perlecan glycosaminoglycan chains were not investigated and may be unlikely, especially as heparan sulfate and other sulfated glycosaminoglycans were found to be relatively resistant to ROS-induced oxidative damage.[43]

Even at high concentrations, ROS failed to depolymerize the EHS matrix entirely. As EHS tumors were grown in lathyritic mice[19] in which lysine-mediated cross-links of collagen were abolished,[12] the question arose as to the biochemical basis of this resistance to ROS-induced disassembly. A simple explanation was provided by the ROS-induced cross-linking of laminin found within the residual in-

soluble matrix. Collectively, these results provided evidence that ROS exert two different, countercurrent effects on the EHS matrix; although they caused partial solubilization, they simultaneously induced cross-linking that presumably counteracts complete disassembly of the matrix meshwork.

Detailed information about ROS-induced formation of molecular cross-links and aggregates was obtained when isolated, soluble laminin/entactin and type IV collagen were incubated with increasing concentrations of ROS. SDS-insoluble oligomers and aggregates consisted primarily of laminin and increased in size and number with the concentrations of ROS. H_2O_2 alone in the absence of Fe^{2+} was also sufficient to induce substantial aggregation. Formation of bityrosine residues was identified as one potential cross-linking mechanism, whereas MDA Schiff bases, a typical product of lipid peroxidation, were not encountered. These data suggest that formation of covalently linked aggregates of matrix proteins *in vitro* was directly mediated by ROS.

These results raised the question of whether a single compound of ROS could be identified as primary cause for the oxidative damage, because the Fenton reaction generates a mixture of different ROS of variable half-life and chemical reactivity. By use of specific scavengers, we have provided evidence that the hydroxyl radical was the most damaging agent for laminin/entactin and type IV collagen. This is in agreement with the known harmful role of the hydroxyl radicals *in vivo*, for example, in development of the proteinuria in puromycin aminonucleoside nephrosis,[44] in experimental arthritis,[45] and in invasion and metastasis of Colon 26-M5 tumor cells.[46] The short-lived hydroxyl radical was found to cause damage especially on proteins that contain metal-binding sites, at which it is locally generated.[33] It remains to be determined whether similar site-directed actions of hydroxyl radicals contribute to ROS-induced conformational changes, aggregations, and fragmentations of EHS matrix proteins.

Can we distinguish between degradative actions of ROS and proteases? This is even more important, as EHS matrix as well as basement membranes are known to contain serine proteases, such as plasmin,[47] and also metalloproteases,[26] which are associated with laminin.[25] Moreover, ROS are known to increase the susceptibility of proteins to degradation by proteases and to activate latent metalloproteases. Several precautions were taken to minimize proteolysis, such as prescreening for protease activity, use of a mixture of protease inhibitors, and incubations in the cold. As indicated by appropriate control experiments, these precautions suppressed any potential proteolytic degradation, and thus it appears that the results obtained were primarily due to direct actions of ROS.

Although the results of this report record major *in vitro* effects of ROS on EHS matrix, the question remains whether similar ROS concentrations also occur *in vivo*. Unfortunately, pathologically relevant *in vivo* concentrations of individual ROS are not known.[48] It is possible that, in certain microenvironments, such as domains of surface membranes of activated neutrophils and macrophages, ROS concentrations could be reached sufficiently high to damage surrounding matrix proteins and facilitate cell migration.

The relevance of ROS in the pathogenesis of various human and experimental diseases that involve alterations of extracellular matrix was underscored by the fact that interventional therapies with ROS scavengers caused dramatic reduction of disease activity. For example, human and murine tumor cells were found to produce ROS that correspond with invasive and metastatic behavior.[29,46] Synovial fluids in human rheumatoid arthritis and in potassium-peroxochromate-induced rat arthritis were found to contain high concentrations of ROS.[45,49] ROS-induced degradation of myocardial matrix in ischemic and inflammatory lesions was presumably involved in progressive ventricular dilatation.[11] Eventually, ROS-mediated damage to the GBM was implicated in the development of proteinuria in several experimental glomerular diseases, such as puromycin nephrosis[50] and presumably also Heymann nephritis.[51] Recently, fragments of laminin were found in relatively high concentrations in human sera and urine in diabetes and after environmental exposure to chlorinated hydrocarbons.[52] As the pathogenesis of these conditions involve ROS production, it remains to be determined whether or not these laminin fragments were released from the GBMs by ROS. Rapid and significant loss of laminin was also observed in tubular basement membranes in post-ischemic, ROS-associated renal failure.[53] ROS could be involved in these situations in detachment and fragmentation of laminin and presumably also other matrix proteins from basement membranes. Their ability to form cross-links of matrix proteins could be of additional functional relevance. As an example, *in vitro* chemical cross-linking of EHS matrix or of isolated GBMs increased their porosity, apparently by alteration of their three-dimensional structure.[54,55]

Matrix damage *in vivo* is presumably a multifactorial process that involves a concerted action of ROS, lipid peroxidation, halidation, NO, proteases, and other noxious systems. The results of this study sug-

gest, however, that direct actions of ROS on matrix proteins are essential components of this scenario. It remains to be determined to what extent ROS-induced partial dissolution and cross-linking of EHS matrix reflect pathological situations *in vivo*.

References

1. Yurchenco PD, Schittny JC: Molecular architecture of basement membranes. FASEB J 1990, 4:1577–1590
2. Schnaper HW, Kleinman HK, Grant DS: Role of laminin in endothelial cell recognition and differentiation. Kidney Int 1993, 43:20–25
3. Aumailley M: Structure and supramolecular organization of basement membranes. Kidney Int Suppl 1995, 49:S4–S7
4. Farquhar MG: The glomerular basement membrane: a selective macromolecular filter. Cell Biology of Extracellular Matrix, ed 2. Edited by ED Hay. New York, Plenum Press, 1991, pp 365–418
5. Abrahamson DR, Vanden Heuvel GB, Clapp WL: Nephritogenic antigens in the glomerular basement membrane. Immunologic Renal Diseases. Edited by EG Neilson, WG Couser. Philadelphia, Lippincott-Raven, 1997, pp 217–234
6. Tryggvason K: Mutations in type IV collagen genes and Alport phenotypes. Contrib Nephrol 1996, 117:154–171
7. Turner N, Mason PJ, Brown R, Fox M, Povey S, Rees A, Pusey CD: Molecular cloning of the human Goodpasture antigen demonstrates it to be the α3 chain of type IV collagen. J Clin Invest 1992, 89:592–601
8. Noakes PG, Gautam M, Mudd J, Sanes JR, Merlie JP: Aberrant differentiation of neuromuscular junctions in mice lacking s-laminin/laminin-β2. Nature 1995, 374: 258–262
9. Kerjaschki D, Neale TJ: Molecular mechanisms of glomerular injury in rat experimental membranous nephropathy (Heymann nephritis). J Am Soc Nephrol 1996, 7:2518–2526
10. Britton RS: Metal-induced hepatotoxicity. Semin Liver Dis 1996, 16:3–12
11. Lonn E, Factor SM, Van Hoeven KH, Wen WH, Zhao M, Dawood F, Liu P: Effects of oxygen free radicals and scavengers on the cardiac extracellular collagen matrix during ischemia-reperfusion. Can J Cardiol 1994, 10:203–213
12. Orkin RW, Gehron P, McGoodwin EB, Martin GR, Valentine T, Swarm R: A murine tumor producing a matrix of basement membrane. J Exp Med 1977, 145:204–220
13. Gutteridge JM: Ferrous-salt-promoted damage to deoxyribose and benzoate: the increased effectiveness of hydroxyl-radical scavengers in the presence of EDTA. Biochem J 1987, 243:709–714
14. Davies KJ: Protein damage and degradation by oxygen radicals. I. General aspects. J Biol Chem 1987, 262:9895–9901
15. Richmond R, Halliwell B, Chauhan J, Darbre A: Superoxide-dependent formation of hydroxyl radicals: detection of hydroxyl radicals by the hydroxylation of aromatic compounds. Anal Biochem 1981, 118:328–335
16. Greenwald RA, Moy WW: Inhibition of collagen gelation by action of the superoxide radical. Arthritis Rheum 1979, 22:251–259
17. Girotti AW, Thomas JP, Jordan JE: Xanthine oxidase-catalyzed crosslinking of cell membrane proteins. Arch Biochem Biophys 1986, 251:639–653
18. Bull C, Fee JA, O'Neill P, Fielden EM: Iron-ethylenediaminetetraacetic acid (EDTA)-catalyzed superoxide dismutation revisited: an explanation of why the dismutase activity of Fe-EDTA cannot be detected in the cytochrome c/xanthine oxidase assay system. Arch Biochem Biophys 1982, 215:551–555
19. Kleinman HK, McGarvey ML, Liotta LA, Robey PG, Tryggvason K, Martin GR: Isolation and characterization of type IV procollagen, laminin, and heparan sulfate proteoglycan from the EHS sarcoma. Biochemistry 1982, 21:6188–6193
20. Thomas CE, Jackson RL: Lipid hydroperoxide involvement in copper-dependent and independent oxidation of low density lipoproteins. J Pharmacol Exp Ther 1991, 256:1182–1188
21. Yurchenco PD, Cheng YS: Laminin self-assembly: a three-arm interaction hypothesis for the formation of a network in basement membranes. Contrib Nephrol 1994, 107:47–56
22. Yurchenco PD, Cheng YS, Colognato H: Laminin forms an independent network in basement membranes [published erratum appears in J Cell Biol 1992 18:493]. J Cell Biol 1992, 117:1119–1133
23. Engel J: Electron microscopy of extracellular matrix components. Methods Enzymol 1994, 245:469–88
24. Riley DP, Rivers WJ, Weiss RH: Stopped-flow kinetic analysis for monitoring superoxide decay in aqueous systems. Anal Biochem 1991, 196:344–349
25. Mackay AR, Gomez DE, Cottam DW, Rees RC, Nason AM, Thorgeirsson UP: Identification of the 72-kDa (MMP-2) and 92-kDa (MMP-9) gelatinase/type IV collagenase in preparations of laminin and Matrigel. Biotechniques 1993, 15:1048–1051
26. Birkedal Hansen H: Proteolytic remodeling of extracellular matrix. Curr Opin Cell Biol 1995, 7:728–735
27. Meier B, Radeke HH, Selle S, Younes M, Sies H, Resch K, Habermehl GG: Human fibroblasts release reactive oxygen species in response to interleukin-1 or tumour necrosis factor-α. Biochem J 1989, 263:539–545
28. Radeke HH, Cross AR, Hancock JT, Jones OT, Nakamura M, Kaever V, Resch K: Functional expression of NADPH oxidase components (α- and β-subunits of cytochrome b558 and 45-kDa flavoprotein) by intrinsic human glomerular mesangial cells. J Biol Chem 1991, 266:21025–21029
29. Szatrowski TP, Nathan CF: Production of large amounts

of hydrogen peroxide by human tumor cells. Cancer Res 1991, 51:794–798
30. Rosen GM, Pou S, Ramos CL, Cohen MS, Britigan BE: Free radicals and phagocytic cells. FASEB J 1995, 9:200–209
31. Kaushal GP, Shah SV: Proteases and oxidants in glomerular injury. Immunologic Renal Diseases. Edited by EG Neilson, WG Couser. Philadelphia, Lippincott-Raven, 1997, pp 397–415
32. Davies KJ, Lin SW, Pacifici RE: Protein damage and degradation by oxygen radicals. IV. Degradation of denatured protein. J Biol Chem 1987, 262:9914–9920
33. Stadtman ER: Oxidation of free amino acids and amino acid residues in proteins by radiolysis and by metal-catalyzed reactions. Annu Rev Biochem 1993, 62:797–821
34. Jarasch ED, Bruder G, Heid HW: Significance of xanthine oxidase in capillary endothelial cells. Acta Physiol Scand Suppl 1986, 548:39–46
35. Parks DA, Granger DN: Xanthine oxidase: biochemistry, distribution and physiology. Acta Physiol Scand Suppl 1986, 548:87–99
36. Weiss SJ: Oxygen, ischemia, and inflammation. Acta Physiol Scand Suppl 1986, 548:9–37
37. Halliwell B, Cross CE: Oxygen-derived species: their relation to human disease and environmental stress. Environ Health Perspect 1994, 102(Suppl 10):5–12
38. Charonis AS, Reger LA, Dege JE, Kouzi Koliakos K, Furcht LT, Wohlhueter RM, Tsilibary EC: Laminin alterations after in vitro nonenzymatic glycosylation. Diabetes 1990, 39:807–814
39. Weiner L, Kreimer D, Roth E, Silman I: Oxidative stress transforms acetylcholinesterase to a molten-globule-like state. Biochem Biophys Res Commun 1994, 198: 915–922
40. Kato Y, Uchida K, Kawakishi S: Oxidative fragmentation of collagen and prolyl peptide by Cu(II)/H_2O_2: conversion of proline residue to 2-pyrrolidone. J Biol Chem 1992, 267:23646–23651
41. Kashihara N, Watanabe Y, Makino H, Wallner E, Kanwar YS: Selective decreased de novo synthesis of glomerular proteoglycans under the influence of reactive oxygen species. Cell Biol 1992, 89:6309–6313
42. Panasyuk A, Frati E, Ribault D, Mitrovic D: Effect of reactive oxygen species on the biosynthesis and structure of newly synthesized proteoglycans. Free Radic Biol Med 1994, 16:157–167
43. Moseley R, Waddington R, Evans P, Halliwell B, Embery G: The chemical modification of glycosaminoglycan structure by oxygen-derived species in vitro. Biochim Biophys Acta 1995, 1244:245–252
44. Thakur V, Walker PD, Shah SV: Evidence suggesting a role for hydroxyl radical in puromycin aminonucleoside-induced proteinuria. Kidney Int 1988, 34:494–499
45. Miesel R, Kroger H, Kurpisz M, Weser U: Induction of arthritis in mice and rats by potassium peroxochromate and assessment of disease activity by whole blood chemiluminescence and 99mpertechnetate-imaging. Free Radic Res 1995, 23:213–227
46. Nonaka Y, Iwagaki H, Kimura T, Fuchimoto S, Orita K: Effect of reactive oxygen intermediates on the in vitro invasive capacity of tumor cells and liver metastasis in mice. Int J Cancer 1993, 54:983–6
47. Mignatti P: Extracellular matrix remodeling by metalloproteinases and plasminogen activators. Kidney Int Suppl 1995, 49:S12–S14
48. Briggs RT, Drath DB, Karnovsky ML, Karnovsky MJ: Localization of NADH oxidase on the surface of human polymorphonuclear leukocytes by a new cytochemical technique. J Cell Biol 1975, 67:566–586
49. Winrow VR, Winyard PG, Morris CJ, Blake DR: Free radicals in inflammation: second messengers and mediators of tissue destruction. Br Med Bull 1993, 49: 506–522
50. Diamond JR, Bonventre JV, Karnovsky MJ: A role for oxygen free radicals in aminonucleoside nephrosis. Kidney Int 1986, 29:478–483
51. Shah SV: Evidence suggesting a role for hydroxyl radical in passive Heymann's nephritis. Am J Physiol 1988, 245:F337–F344
52. Price RG, Taylor SA, Crutcher E, Bergamaschi E, Franchini I, Mackie AD: The assay of laminin fragments in serum and urine as an indicator of renal damage induced by toxins. Toxicol Lett 1995, 77:313–318
53. Lin JJ, Partin J, Kaskel FJ: Changes in laminin during recovery from postischemic acute failure in rats. Exp Nephrol 1996, 4:279–285
54. Walton HA, Byrne J, Robinson GB: Studies of the permeation properties of glomerular basement membrane: cross-linking renders glomerular basement membrane permeable to protein. Biochim Biophys Acta 1992, 1138:173–183
55. Boyd White J, Williams JC Jr: Effect of cross-linking on matrix permeability: a model for AGE-modified basement membranes. Diabetes 1996, 45:348–353